FUDMA Journal of Sciences (FJS)
ISSN online: 2616-1370
ISSN print: 2645 - 2944
Vol. 7 No. 3, June, 2023, pp 293 - 303
DOI: https://doi.org/10.33003/fjs-2023-0703-1967

ROLE OF SUCTION/INJECTION ON MIXED CONVECTION FLOW IN A VERTICAL MICROCHANNEL FILLED WITH POROUS MATERIAL

[1]Deborah A. Daramola, [2]Abiodun O. Ajibade, [3]Hammed. A. Lawal

[1]Department of Mathematics, Air-Force Institute of Technology Kaduna, Nigeria
[2]Department of Mathematics, Ahmadu Bello University, Zaria, Nigeria
[3]Department of Physics, Air Force Institute of Technology, Kaduna, Nigeria

*Corresponding authors' email: debola32000@yahoo.com

ABSTRACT

A suction/injection controlled mixed convection flow of an incompressible and viscous fluid in a vertical microchannel filled with porous material with asymmetric plate temperature is presented. The governing equations are derived and solved using the method of undetermined coefficient. The closed form expression for temperature field, velocity field, skin friction and Nusselt number for the steady fully developed flow are obtained analytically. The effects of the governing parameters on the microchannel hydrodynamic and thermal behaviors are determined. It is interesting to point out that growing the Darcy number as well as the suction S accelerate the fluid motion while they reduce the critical values of the $\frac{Gr}{Re}$ (at which flow reversal sets in) on both plates. The stability of the flow is affected by variation in the permeability of the porous material.

Keywords: vertical microchannel, mixed convection, temperature jump, velocity slip, porous media, suction, injection

INTRODUCTION

Fluid flow and heat transfer in micro devices have received considerable attention during the past decade due to its many applications in microelectromechanical systems (MEMS) and biomedical applications systems technology. Microfluidics devices are characterized by their small length scale ($< 1\mu m$) e.g. sensors, ducts, turbines, actuators, valves and pumps. Therefore the phenomenon of wall slip becomes increasingly important as the characteristic channel width becomes comparable with the molecular mean free path. The small dimension encounter in microfluidic can result in gas rarefaction. Knudsen number, Kn defines the ratio of the molecular mean free path to the characteristic channel width, and is also used to measure the degree of rarefaction of gases encounter in such small length scale flow and to measure the degree of validation of the continuum model. Beskok and Karniadakis (1999) gives a classification of different gas flow regimes as follows $\mathrm{Kn} < 0.001$for continuum flow, $0.001 < Kn < 0.1$for slip flow.

Several studies have been carried out in field of micro geometry flow since the early work of Tuckerman and Pease (1981). Garimella and Lee (2006) studied the thermally developing flow and heat transfer in rectangular microchannels of different aspect ratio. Chen and Weng (2005) analytically studied the fully developed natural convection in an open-ended vertical parallel plate microchannel with asymmetric wall temperature distributions in which the effects of rarefaction and fluid-wall interaction were shown to increase the volume flow and to decrease the heat transfer rate. Forced convection in slightly curved microchannels is studied by Wang and Liu (2007).

The application of combined convection heat and mass transfer arises in a lot of engineering devices such as heat exchangers, solar collectors and nuclear reactors. Several authors have investigated fluid flows involving the combined effect of free and forced convections in different flow geometries. Avci and Aydin (2007a) analysed mixed convection of rarefied gas in a vertical asymmetrically heated microchannel. The work concluded that increase in rarefaction is found to decrease the Nusselt number, while increase in $\frac{Gr}{Re}$leads to increase in the Nusselt number. In another work, Avci and Aydin (2007b) analysed the mixed convection in a vertical parallel plate microchannel with asymmetric plate heat fluxes. The work also revealed that the Nusselt number decreases as Kn increases. Other notable works on mixed convection flow include Wen-Mon and Hung-Yi (2001) and Kou and Lu (1993). Avramenko *et al.* (2017) investigates into mixed convection in a vertically oriented microchannel with slip bound conditions, it was discovered that the Knudsen number entails heat transfer deterioration except for $\Pr = 10$ and high Rayleigh number as well diminishes the hydraulic resistance for low Rayleigh number.

Gas flow in a porous medium have been of great importance in packed bed catalytic reactor, geothermal reservoirs, drying of porous solid, petroleum resources and many others. Many researchers used porous material to enhance heat transfer in both internal and external fluid flow situation. Kaviany (1985) presented an analytical solution of the transport equations based on the Brinkman-extended Darcy flow model. Vafai and Kim (1989) also presented a closed form solution of the Brinkman-Forchhemier-extended Darcy momentum equation and the associated heat equation for the case of a fully developed flow with heat flux at the boundary. The analysis was limited to the case of effective viscosity equal to the fluid viscosity. Renken and Poulikakos (1988) employed a finite difference formulation of the differential equations this allows for viscosity variations and able to deal with developing flow. Haddad *et al.* (2006) investigated the hydrodynamic and thermal behaviour of gas flow in a microchannel filled with porous media. It was found that the skin friction and Nusselt number both increase by increasing Darcy number and decreasing Knudsen number. Kuznetsov (1998, 2009) investigated the study of fluid flow and heat transfer during forced convection in a composite channel partly filed with a Brinkman-Forchheimer porous medium. He also studied forced convection with slip flow in a channel or duct occupied by a hyper-porous medium saturated by a rarefied gas and found that velocity slip leads to increase heat transfer while temperature slip leads to decrease in heat transfer. Hadim and Chen (1984) also investigated the Darcy number effects on the buoyancy-assisted mixed convection in the entrance region of a vertical channel with asymmetric heating at fixed values of Reynolds number, Forchheimer number and Prandtl number. It is found that as the Darcy number is decreased, there exists increase in heat transfer. Mishra *et al.* (2002) investigated mixed convection flow in a porous medium bounded by two vertical plates; it is found that the flow is parabolic for higher Darcy number whereas there is a reverse type of motion for lower Darcy numbers. Jha *et al.* (2012) studied steady fully developed mixed convection flow in a vertical parallel plate microchannel;it is found that critical values of the mixed convection parameter $\frac{Gr}{Re}$ (which led to flow reversal) decrease as Darcy number increase. Abdullah *et al.* (2019) studied the effect of a porous medium on flow and mixed convection heat transfer of nanofluids with variable properties in a trapezoidal enclosure and it as found that the average Nusselt number increases by increasing Darcy number. Rouhollah (2021) investigate the combined effects of a microchannel with porous media and transverse vortex generators (TVG) on convective heat transfer performance, it was discovered that the use of porous medium in the microchannel increases friction due to significant reduction of pore radius in the porous medium, therefore the fluid overcoming the permeation loss of the porous media in the microchannel. Ajibade *et al.* (2022) studied analytically the combined effect of viscous and darcy dissipation on Mixed convection flow in a composite vertical channel partially filled with porous material. Somayeh *et al.* (2022) numerically studied the effect of microchannel-porous media and nanofluid on temperature and performance of CPV system, it was discovered that the thermal behaviour of the microchannel with porous layer varies with the change of Darcy number.

Among the reviewed articles on mixed convection, of interest to us is the work of Aydin and Avci (2007) which considered mixed convection in vertical microchannel. However, there are several flows in practice that involve porous media applications. For instance, modelling of fluid flows in food storage, insulation building, storage of nuclear waste materials, underground draining and oil extraction amongst others. In such flow situations, results from Aydin and Avci (2007) is not readily applicable therefore this work is aimed at investigating such flows when the microchannel is filled with porous materials.

Suction and injection play a significant role in the control of flow past an infinite plate or within parallel plates. Their application is in practical problems in the field of aerodynamics, environmental application and space science. The flow control on a subsonic airfoil by suction and injection was studied by Shojaefard *et al.* (2005). It is concluded that suction increases the lift coefficient while injection reduces the skin friction which invariably reduce the energy consumption during flight of subsonic aircraft. Jha and Ajibade (2010) studied free convective flow between vertical porous plates with periodic heat input; it is observed that temperature is higher near the plate with injection, while velocity is more enhanced near the plate with suction. Jha and Ajibade (2009) investigated the free convective flow of heat generating/absorbing fluid between vertical porous plates with periodic heat input, they observed that the influence of heat sink is suppressed by large suction values and influence of suction/injection is suppressed by large value of heat sink. Al-Nimr and Alkam (2000) investigated the transient flow in porous slabs with suction and injection, it is found that suction decreases the axial velocity. Sheremetet *et al.* (2018) examine mixed convection heat transfer in a square porous cavity filled with nanofluid with suction/injection effect, they numerically studied the effect of the sizes of inlet and oulets zones, Darcy number, rayleigh number on the nanofluid flow and heat transfer pattern. It was found that increase in the sizes of the inlet and outlet zones characterises an essential cooling of the cavity with less essential diminution of the nanoparticle volume fraction in the upper left corner. Jha and Babatunde (2018) investigate the role of suction\injection on steady fully developed mixed convection flow in a vertical parallel plate microchannel. It was discovered that as suction/injection at the micro-porous channel surface increases, the volume flow rate increases while the rate of heat transfer decrease.

In all the works mentioned above, none was found to investigate the effect of suction/injection on the mixed convection in a microchannel filled with porous material.

In the present work, the role of suction/injection on mixed convection flow in a microchannel filled with porous material is examined. Fully developed mixed convection flow is considered because the study of such flows gives the limiting condition for developing flows and provides an analytical check on numerical solutions. Exact solution obtained in this work serves as accuracy checks for experimental and asymptotic methods. This results can be validated with Jha and Babatunde (2018) when the permeability is large.

MATERIALS AND METHODS

Mathematical Analysis

Considering a steady laminar mixed convective flow of a viscous incompressible fluid in a vertical microchannel formed by two infinite vertical porous parallel plates. The porous plates are taken vertically at $y' = \pm W$, the fluid flow being parallel to the x-axis which is opposite to the gravitational acceleration vector g . The porous plates are held at different uniform temperature as shown in Figure.1. The channel is filled with porous material. The fluid is assumed to be in local thermal equilibrium. The porous medium is assumed to be homogenous and isotropic. In addition, the flow is subjected to suction of the fluid from one plate $(y' = -W)$and in order to conserve the mass of the fluid in the channel, fluid is being injected into the channel at the same rate through the other plate $(y' = +W)$. The flow is assumed to be hydrodynamically as well as thermally fully developed.

We consider a two dimensional flow so that $\vec{V} = (u, v, 0)$ where u and v are the vertical and horizontal components of the velocity respectively. Moreover, it is assumed that the flow is along the x-axis , so that only the x-component of $V$the velocity vector does not vanish but horizontal velocity $v = V_0$remains constant, which is the velocity of suction/injection. Applying the Boussinesq approximation, where all the fluid properties except density in the buoyancy term are considered as constant.

$$\frac{\partial u'}{\partial x'} = 0, \frac{\partial v'}{\partial y'} = \frac{dv'}{dy'}, \mathrm{v} = \mathrm{V}_0 = \text{const}, \tag{1}$$

$$\frac{\partial p}{\partial x} = \frac{dp'}{dx'} = const, \frac{\partial T'}{\partial x'} = 0,$$

In this study, the usual continuum approach is coupled with the two main characteristics of the microscale phenomena, the velocity slip and the temperature jump. Velocity slip is defined as [1]

$$u_s = -\frac{2-F}{F}\lambda \frac{\partial u'}{\partial y'}|y' = \pm W, \tag{2}$$

where u_s is the slip velocity; λ is the molecular mean free path; and F is the tangential momentum accommodation coefficient, and the temperature jump is defined as [1],

$$T_s - T_W = -\frac{2-F_t}{F_t}\frac{2\zeta}{\zeta+1}\frac{\lambda}{Pr}\frac{\partial T'}{\partial y'}|y' = \pm W, \quad (3)$$

where T_s is the temperature of the gas at the plate; T_W is the plate temperature; and F_t is the thermal accommodation coefficient.

A model that combines the Navier-Stoke equations with a slip flow boundary condition have been reported by Arkilic *et al.* (1994) to give reasonably good agreement with experimental data.

Using the extended Darcy-Brinkman combined with the Navier-Stokes equation to model the flow in the porous medium and the velocity slip and temperature jump condition at the boundary to model the gaseous slip in the microchannel. Since convection flow in microchannel is of low Reynold number (Purcell (1977)) therefore viscous dissipation term is negligible relative to the $\frac{d^2T}{dy^2}$, also the effect of compressibility for this typically low-speed microflow is negligible (Kavehpour *et al.* (1997).) Based on the flow assumption in eq. (1) above, the momentum equation for the y-axis vanishes due to the assumption of a constant transpiration velocity $(v = V_0)$ which results in:

$$\frac{dp'}{dy'} = 0. \quad (4)$$

The conservation equations for momentum and energy can be shown to take the form:

Momentum equation:

$$V_0\frac{du'}{dy'} = \nu_{eff}\left(\frac{d2u'}{dy'2}\right) + g\beta(T' - T_0) - \frac{1}{\rho}\frac{dp'}{dx'} - \frac{\nu}{K}u', \quad (5)$$

Energy equation:

$$V_0\frac{dT'}{dy'} = \left(\frac{\kappa}{\rho c_p}\right)\frac{d^2T'}{dy'^2}, \quad (6)$$

In eqns. (5) and (6), V_0 is the constant normal velocity on the microchannel surfaces.

Where ν and ν_{eff} are the kinematic viscosity velocity and the effective kinematic viscosity velocity respectively, g is the gravitational acceleration and K is the permeability of the porous medium.

The boundary condition for the flow in the present problem is given as:

$$u' = u_{s1},\ T' = T_{s1},\ \text{at}\ y' = -W, \quad (7)$$
$$u' = u_{s2},\ T' = T_{s2},\ \text{at}\ y' = W$$

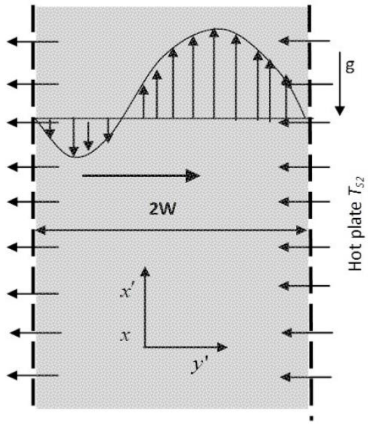

Figure 1: Schematic Diagram of the flow

By introducing the following non dimensional quantities

$$y = \frac{y'}{W},\quad x = \frac{x'}{ReW}, \theta = \frac{T'-T_0}{T_1-T_0}, U = \frac{u'}{u_0}, Kn = \frac{\lambda}{W}, S = \frac{V_0W}{\nu}, \quad (8)$$
$$Da = \frac{K}{W^2}, M = \frac{\nu_{eff}}{\nu}, p = \frac{p'}{\rho u_0^2}, Gr = \frac{g\beta(T_1 - T_0)W^3}{\nu^2}, Re = \frac{u_0W}{\nu},$$

Eqns. (5) and (6) are presented in the dimensionless form as:

$$M\frac{d^2U}{dy^2} + S\frac{dU}{dy} - \frac{U}{Da} = \frac{dp}{dx} - \frac{Gr}{Re}\theta, \quad (9)$$

$$\frac{d^2\theta}{dy^2} + SPr\frac{d\theta}{dy} = 0, \quad (10)$$

The 2nd term on the R.H.S of Eqn. (9) represents the mixed convection term while $\frac{Gr}{Re}$ is the mixed convection parameter. Large values of $\frac{Gr}{Re}(Gr \gg Re)$ represents flow driven by natural convection while small value of $\frac{Gr}{Re}(Gr \ll Re)$ give rise to forced convection flow. Moderate values of $\frac{Gr}{Re}$, represent a mixed convection flow where contributions of both the pressure gradient and buoyancy assistance are significant.

In term of the dimensionless variables defined in eqn. (8), boundary conditions given in eqn.(7) can be shown as:

$$\theta = \frac{T_{s1}-T_0}{T_1-T_0} = r_\tau + \beta_\tau Kn\frac{d\theta}{dy},\quad U = \beta_\tau Kn\frac{dU}{dy} at y = -1, \quad (11)$$

$$\theta = \frac{T_{s2}-T_0}{T_1-T_0} = 1 - \beta_\tau Kn\frac{d\theta}{dy}, U = -\beta_\tau Kn\frac{dU}{dy} at y = 1.,$$

where Pr is the Prandtl number which is inversely proportional to the thermal diffusivity of the working fluid, Kn is the ratio of the mean free path of the fluid to the characteristic length of the flow domain, M is the ratio of the effective viscosity of the porous media to the viscosity of the fluid, Da is the Darcy number, where S is the dimensionless suction/injection parameter. Positive values of S indicate suction through the plate $y = -1$ with a simultaneous injection on the plate $y = 1$ while negative of S indicate suction through the plate $y = 1$ with a simultaneous injection on the plate $y = -1$.

$$r_\tau = \frac{T_1-T_0}{T_2-T_0}, \quad (12)$$

solving eqn. (10) and applying the boundary conditions, eqn.(11) gives:

$$\theta(y) = C_1 + C_2exp(-SPry), \quad (13)$$

Where,

$C_1 = 1 + \left(\frac{r_\tau - 1}{2SPr\beta_\tau Kncosh(SPr) + sinh(SPr)}\right)(SPr\beta_\tau Kn - 1)exp(-SPr),$ (14)

$C_2 = \frac{r_\tau - 1}{2SPr\beta_\tau Kncosh(SPr) + sinh(SPr)},$

Substituting, eqn. (13) into the momentum equation eqn. (9) and solving with the boundary condition in eqn. (11) gives$U(y) = exp\left(\frac{-Sy}{2M}\right)\left(C_3cosh(a_1y) + C_4sinh(a_1y)\right) - Da\frac{dp}{dx} +$

$\frac{Gr}{Re}\left(DaC_1 - \left(\frac{C_2}{x_1M}\right)\left(exp(-SPry)\right)\right),$ (15)

where the constants used in eqn.(15) are defined below in the appendices,

At any cross section in the channel, the dimensionless mean velocity U_m can be written as:

$U_m = \int_{-1}^{1} U\,dy = 2,$ (16)

Substituting eqn. (15) into eqn.(17) gives

$\frac{dp}{dx} = \frac{2 - \frac{Gr}{Re}x_{11}}{x_{12}},$ (17)

The rate of heat transfer, the Nusselt number, Nu on the boundary plates of the microchannel, is respectively

$Nu|_{y=-1} = \frac{d\theta}{dy}|_{y=-1} = -SPrC_2exp(SPr),$ (18)

$Nu|_{y=1} = \frac{d\theta}{dy}|_{y=1} = -SPrC_2exp(-SPr),$

The expression for the critical value of $\frac{Gr}{Re}$ after which reverse flow sets in, is obtained by setting $\frac{du}{dy} = 0$ This is given on both walls by the expressions below

$\frac{Gr}{Re}|_{y=-1} = \frac{2x_{16}}{x_{11}x_{16} - x_{17}x_{12}},$ (19)

$\frac{Gr}{Re}|_{y=1} = \frac{2x_{21}}{x_{11}x_{21} - x_{22}x_{12}},$

The expression for the skin friction on both plates are as follow

$\tau_{-1} = \frac{du}{dy}|_{y=-1},$

$= \frac{S}{2M}\left(exp\left(\frac{S}{2M}\right)\left(C_3cosh(a_1) - C_4sinh(a_1)\right) + a_1exp\left(\frac{S}{2M}\right)\left(C_4cosh(a_1) - C_3sinh(a_1)\right)\right)$

$+ \frac{\frac{Gr}{Re}C_2SPrexp(SPr)}{x_1M},$

$\tau_1 = \frac{du}{dy}|_{y=1}$

$= \frac{-S}{2M}\left(exp\left(\frac{-S}{2M}\right)\left(C_3cosh(a_1) + C_4sinh(a_1)\right) + a_1exp\left(\frac{-S}{2M}\right)\left(C_4cosh(a_1) + C_3sinh(a1)\right)\right)$

$+ \frac{\frac{Gr}{Re}C_2SPrexp(-SPr)}{x_1M}$ (20)

RESULT AND DISCUSSION

The present work investigates the fluid flow in a microchannel formed by two infinite vertical parallel porous plates held at different uniform temperature filled with porous material. The influence of the mixed convection parameter, $\frac{Gr}{Re}$, the Knudsen number, Kn the ratio of the plate temperature, r_τ, the Darcy number, Da, the suction and injection parameter Son the microchannel hydrodynamic and thermal behavior are highlighted in the course of the investigation. The Knudsen number, Kn which measures the ratio of the mean free path of the fluid to the characteristic length of the flow domain and degree of the validity of the continuum, velocity slip parameter β_v and temperature jump β_τ. In the present work, the values of β_v used is unity while the value of β_τ is taken to be 1.667 corresponding to the temperature jump for air [1]. The value of Prandtl number Pr used is 0.71, the ratio of viscosities M is unity, while the Knudsen number values in the range of $(0.01 \leq Kn \leq 0.1)$ are used since there exists slip flow regime as discussed by Avci and Aydin [6]. The ratio of the plate temperature difference $r_\tau = 0.2$ is used, the mixed convection parameter $\frac{Gr}{Re}$ values in the range $-350 \leq \frac{Gr}{Re} \leq 300$ are used. The suction/ injection values are in the range $(-2 \leq S \leq 2)$. For the purpose of discussion, some numerical calculations are carried out and the results of the numerical calculations are presented graphically in figures 2-13.

The present work is validated by comparing limiting result with those available in the existing literature. For large values of Da and taking limiting value of S to be zero, the velocity and temperature distribution given in eqns. (13) and (14) are exactly identical to those given in Avci and Aydin [6].

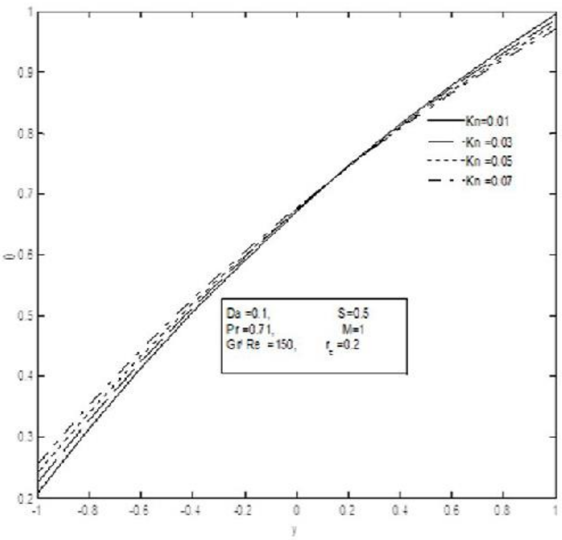

Figure 2: Temperature profile for different Kn

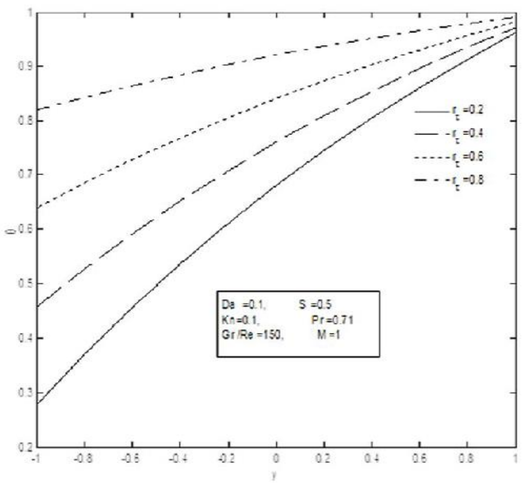

Figure 3: Temperature profile for different r_τ

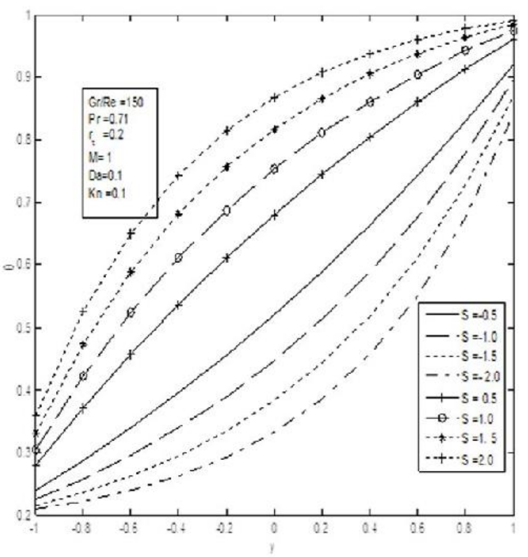

Figure 4: Temperature profile for different S

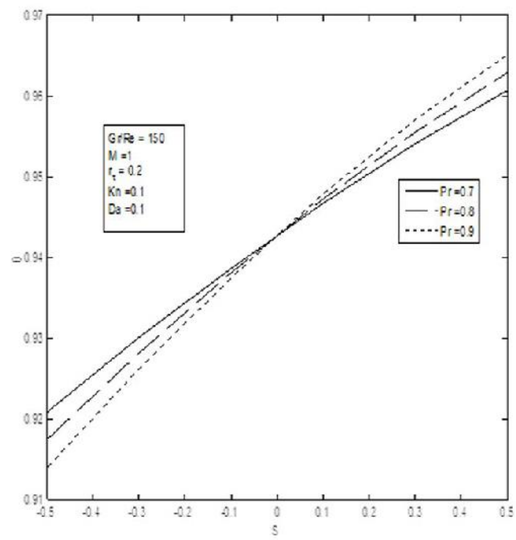

Figure 5: Cross-Sectional temperature variation of S and Pr

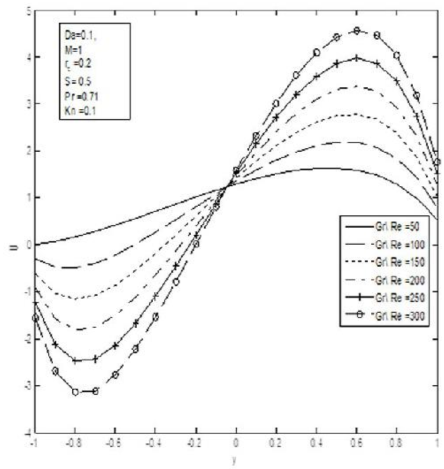

Figure 6: Velocity profile for different $\frac{Gr}{Re}$

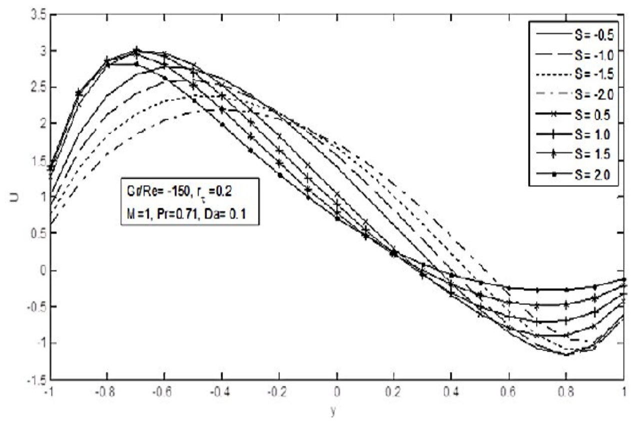

Figure 7:Velocity profile for different S

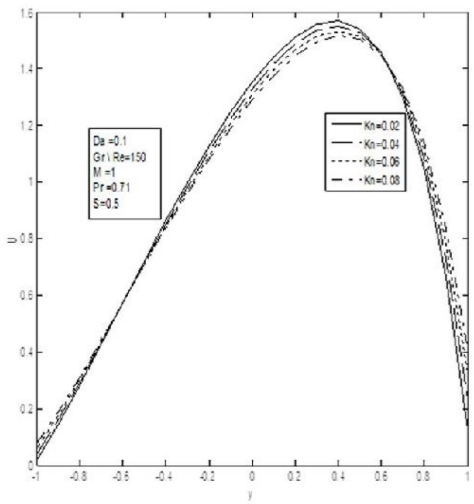

Figure 8: Velocity profile for different Kn

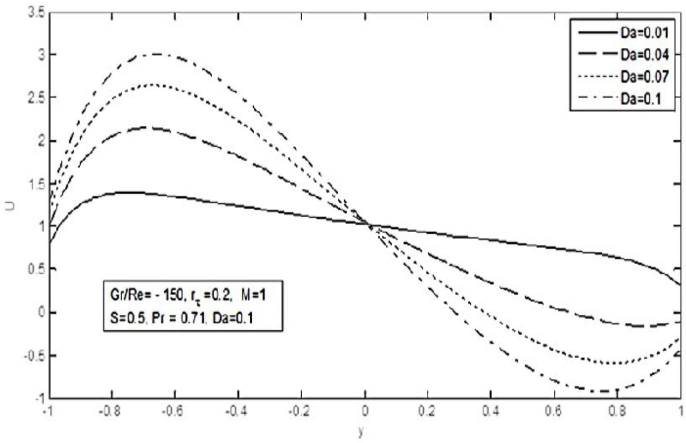

Figure 9: Velocity profile for different Da

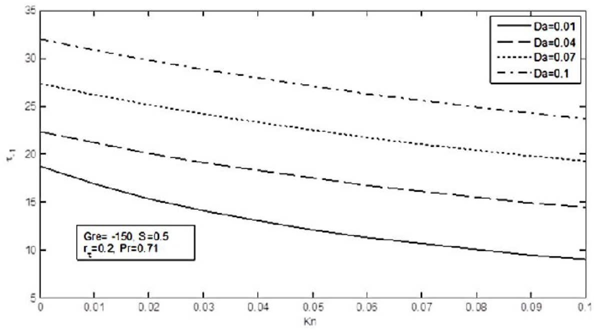

Figure 10: The variation of skin friction and Da at (y=-1)

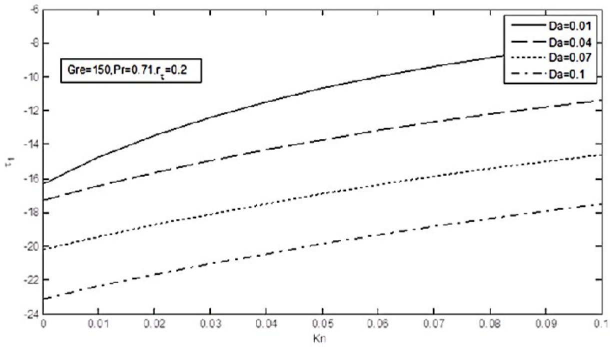

Figure 11: The variation of skin friction and Da at (y=-1)

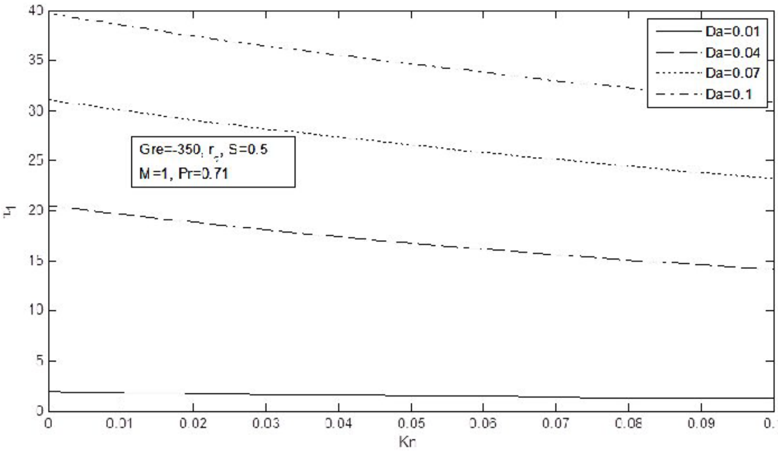

Figure 12: The variation of skin friction and Da at (y=1)

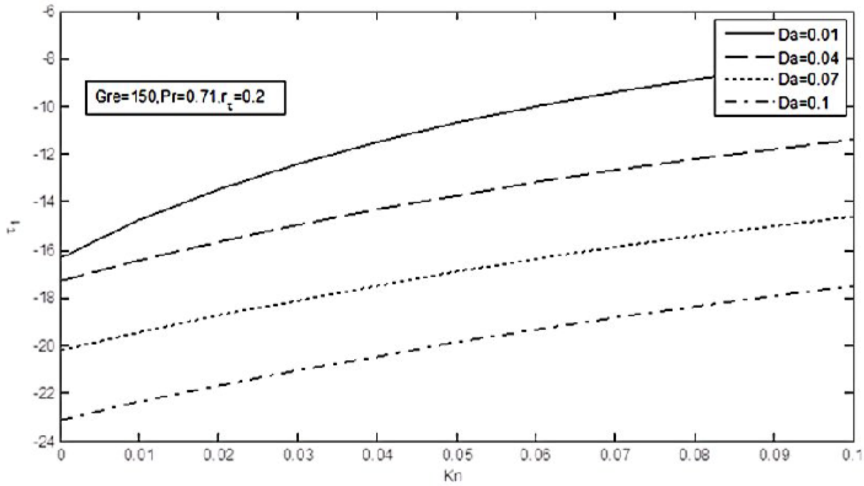

Figure 13: The variation of skin friction and Da at (y=1)

Table 1: Variation of the critical values of $\frac{Gr}{Re}$ with Kn,Da, S ($Pr = 0.71, r_{\tau} = 0.2$)

Da	Kn	S	$\frac{Gr}{Re\|y=-1}$	$\frac{Gr}{Re\|y=1}$
0.001	0.01	-0.5	3037.4	-2421.5
		-0.3	2887.7	-2519.8
		0.3	2519.8	-2887.7
		0.5	2421.5	-3037.4
	0.1	-0.5	3439.2	-2751.5
		-0.3	3261.5	-2852.0
		0.3	2852.0	-3261.5
		0.5	2751.5	-3439.2
0.01	0.01	-0.5	348.64	-282.62
		-0.3	332.13	-292.73
		0.3	292.75	-332.13
		0.5	282.62	-348.64
	0.1	-0.5	383.23	-313.09
		-0.3	364.52	-322.81
		0.3	322.81	-364.52
		0.5	313.09	383.23
0.1	0.01	-0.5	58.15	-50.11
		-0.3	55.83	-51.06
		0.3	51.06	-55.83
		0.5	50.11	-58.15
	0.1	-0.5	61.03	-53.13
		-0.3	58.53	-53.86
		0.3	53.86	-58.53
		0.5	53.13	-63.03

Table 2: Nusselt number as a function of $Kn, Prandattheplatey = -1$($Da = 0.001, r_{\tau} = 0.2$)

Kn	S	$Pr(0.7)$	$Pr(0.8)$	$Pr(0.9)$	$Pr(1.0)$
0.001	-0.5	0.2757	0.2607	0.2462	0.2324
	-0.3	0.3213	0.3111	0.3012	0.2914
	0.3	0.4890	0.5028	0.5168	0.5310
	0.5	0.5552	0.5801	0.6056	0.6317

0.01	-0.5	0.2715	0.2566	0.2423	0.2287
	-0.3	0.3165	0.3064	0.2966	0.2870
	0.3	0.4817	0.4952	0.5090	0.5230
	0.5	0.5467	0.5711	0.5960	0.6216
0.1	-0.5	0.2354	0.2221	0.2094	0.1972
	-0.3	0.2753	0.2664	0.2577	0.2492
	0.3	0.4190	0.4305	0.4422	0.4540
	0.5	0.4740	0.4944	0.5151	0.5361

Table 3: Nusselt number as a function of Kn, Pr and S at the plate $y = 1(Da = 0.001, r_\tau = 0.2)$

Kn	S	$Pr(0.7)$	$Pr(0.8)$	$Pr(0.9)$	$Pr(1.0)$
0.001	-0.5	0.5552	0.5801	0.6056	0.6317
	-0.3	0.4890	0.5028	0.5168	0.5310
	0.3	0.3213	0.3111	0.3012	0.2914
	0.5	0.2757	0.2607	0.2462	0.2324
0.01	-0.5	0.5467	0.5711	0.5960	0.6216
	-0.3	0.4817	0.4952	0.5090	0.5230
	0.3	0.3165	0.3064	0.2966	0.2870
	0.5	0.2715	0.2566	0.2423	0.2287
0.1	-0.5	0.4740	0.4944	0.5151	0.5361
	-0.3	0.4190	0.4305	0.4422	0.4540
	0.3	0.2753	0.2664	0.2577	0.2492
	0.5	0.2354	0.2221	0.2094	0.1972

In Figure. 2, the temperature variation within the fluid domain is presented for different values of Kn. As Kn increases, the fluid rarefaction becomes more pronounced, thereby reducing the fluid-plate interaction on the plates, there is an increase in temperature jump on the channel plates. Consequently the temperature gradient decreases on both plates. However, it is observed from the figure, that temperature is insensitive to Kn at the middle of channel which shows that the influence of temperature jump diminishes from the plates into the channel. Figure 3 is a display of variation of temperature with different values of r_τ, it is seen that increasing r_τ increases the temperature within the channel. However there is higher temperature gradient on the plate $y = 1$ in comparison to the plate at $y = -1$. For $r_\tau = 1$, there is symmetric thermal boundary condition, therefore the asymmetric behaviour of fluid flow is dependent only on the influence of suction and injection. Figure 4 presents the temperature variation for different values of suction and injection. For ($S > 0$) which signifies suction on the plate $y = -1$ and there is a corresponding injection on the plate$y = 1$. It is observed that as suction increases on the plate $y = -1$, there is increase in temperature while the result is just the reverse in case of injection. This is as a result of heat influx into the fluid from the heated plate y= 1. In Figure. 5 the cross-section temperature variation inside the fluid is presented for different values of S and Pr. For ($S > 0$) which is suction on the plate y=-1 and there is a corresponding injection on the plate y =1, there is increase in temperature while as Pr increases, there is a decrease in temperature but the combined effect led to an increase in temperature as Pr increases, while the reverse is the case for injection. However for (S =0) the influence of Pr is absent on the flow.

Figure 6 shows spatial variation of velocity distribution for different values of $\frac{Gr}{Re}$. From this figure, it is observed that increasing $\frac{Gr}{Re}$ increases the fluid velocity near the plate y=1, this is because increase in $\frac{Gr}{Re}$ leads to increase in buoyancy, this act as an aiding effect on the forced flow on the plate y =1, while the velocity decreases near the plate y=-1 as a result of increasing $\frac{Gr}{Re}$ having an opposing effect on the forced flow on the plate y =-1. Figure 7 shows the spatial distribution of velocity for different values of suction and injection. For (S>0) which signifies suction on the plate y= -1 with a corresponding injection on the plate y= 1. An increases in suction which is increase in (S>0) on the plate y= -1, the fluid velocity is observed to increase. It is also observed that when S<0, fluid motion decreases near the plate. However, the trend is reversed towards the channel center when fluid motion decreases as S>0 increases, as well increases as S<0 increases. In Figure. 8, there is a representation of velocity variation for different values of Kn. Increasing values of Kn causes an increase in the velocity slip on both the plates. As Kn increases, the maximum velocity decreases, while the influence of Kn is minimal near the centerline of the channel. Figure 9 shows the variation of velocity with different values of Darcy number Da. It is seen that increasing Darcy number Da increases velocity and this also leads to an increase in the reverse flow velocity near the plate y =1. However, the effect of Darcy number Da is negligible at centerline. It is noteworthy that as Darcy number Da increases, permeability increases. In Figures. 10, 11, 12 and 13 the variation of the skin friction with Da and Kn at the plate y=-1 and y=-1 respectively are shown. It is seen that increase in Da leads to increase in skin friction if the choice of $\frac{Gr}{Re}$ is below the critical value of $\frac{Gr}{Re}$ (value at which reverse flow set in) while an increase in Darcy number Da brings about a reduction in the skin friction if the $\frac{Gr}{Re}$ is higher than the critical value of $\frac{Gr}{Re}$.

Table 1 shows the influence of the different flow parameters on the critical values of $\frac{Gr}{Re}$ after which flow reversal sets in. From the table, it is observed that as suction S increases, there is a decrease in the critical values of $\frac{Gr}{Re}$ on both plates. However, an increase in Kn increases the critical values of $\frac{Gr}{Re}$ on the plate y = -1 but decreases the critical values on the plate y = 1. This is physically true, because as Kn increases, temperature gradient increases near the cold plate and heat transfer is enhanced while the result is just the reverse near the hot plate. In addition, the effect of Da on the critical values of $\frac{Gr}{Re}$ shows that there is a decrease in the critical values of $\frac{Gr}{Re}$ on the plate y=1 and an increase on the plate y =-1. This trend becomes possible because an increase in Da enhances the fluid motion and hence the contribution of the mixed convection parameter towards reverse flow is minimal.

In Tables 2 and 3 it is observed that Nusselt number decreases with increasing values of Prandtl number in the presence of injection on the plate y=-1 (S<0), while it increases with corresponding increase in values of Prandtl number when there is suction through the plate y=-1 (S>0). The nature is just contrast at y =1. Also, for any fixed Prandtl number value, Nusselt number is observed to decrease on both plates as injection (S<0) is increased through the plate y=-1 while it is found to increase as suction (S>0) is increased through the plate y=-1

CONCLUSION

The conclusion of the present work is that suction/injection plays an important role in controlling fluid flow within the channel as it increases the fluid velocity. Also increase in Darcy number is found to decrease the critical values of the $\frac{Gr}{Re}$ (after which flow reversals sets in), thereby reducing the flow stability. The choice of $\frac{Gr}{Re}$ leads to the varying effect of Darcy number Da on the skin friction. This is also decreases as the Knudsen number Kn increases, this is as a result of rarefaction which decreases the fluid- plate interaction. Darcy number can be use to regulate flow motion. Increasing suction/injection parameter, increases the skin friction. Finally, Nusselt number Nu decreases with increase in Knudsen number Kn.

REFERENCES

Abdullah, A.A.A.Al-Rashed, Ghanbar , AliShermal heikhzadeh Alireza Aghaei, Farhad Monfared, Amin Shahsavar Masovd Afrand,(2019), Effect of a porous medium on flow and mixed convection heat transfer of nanofluids with variable properties in a trapezoidal enclosure. Journal of thermal Analysis and Calorimetry 139. 741-754

Abiodun, O. Ajibade, Basant, K. Jha, Jeremiah, Jerry. Gambo (2022),Combined effect of viscous and darcy dissipation on mixed convection flow in a composite vertical channel partially filled with porous material: Analytical Approach, International Communication in Heat and Mass Transfer

Al-Nimr,M. A., and Alkam,M. K., (2000), Basic Fluid Flow Problems in Porous Media, Journal of Porous Media, 3, 45-49.

Arkilic B.Errol., Schmidt, M., and Breuer, K., (1994), Gaseous flow in Microchannels, Application of Micro-fabrication to Fluid Mechanics, ASME, New York,ASME FED-Vol 197 57-66.

Avci, M., and Aydin,O., (2007), Mixed Convection in a Vertical Parallel Plate Microchannel, Trans. ASME - J. Heat Transfer, 129, 162-166

Avci,M., and Aydin, O., (2007), Mixed Convection in a Vertical Parallel Plate Microchannel with Asymmetric Plate Heat Fluxes, Trans. ASME- J. Heat Transfer, 129 1091-1095.

Avramenko, A.A., Tyrinov, A.I., Shevchuk,I.V., Dmitrenko, N.P.,Kravchuk,A.V.,Shevchuk, V.I.(2017), Mixed Convection in a vertically flat micrchannel with slip boundary condition, International Journal of Heat and Mass Transfer, 106 1164-1173

Beskok,A., and Karniadakis, G.E., (1999), A model for flows in channels, pipes and ducts at micro and nanoscales, Microscale Thermophys. Eng., 3, 43-77.

Chen,C.K., and Weng, H.C., (2005), Natural convection in a vertical Microchannel, J.Heat Transfer, 127, 1053-1056.

Gamimella,S.V., and Lee, P.,(2006), Thermally developing flow and heat transfer in rectangular microchannels of different aspect ratios, Int.J.Heat Mass Transfer 49(17) 3060-3067

Haddad,O.M., Al-Nimr, M.A., and Taamneh,Y., (2006), Hydrodynamic and Thermal Behavior of Gas Flow in Microchannels Filled with Porous Media, Journal of Porous Media, 9, 403-414.

Hadim, A., and Chen, G., (1994),Non-Darcy Mixed Convection in a vertical porous channel, J. Thermophys and Heat Transfer, 8, 805-808.

Jha,B.K., and Ajibade,A.O.,(2009) Free convective flow of heat generating/absorbing fluid between vertical porous plates with periodic heat input, Int. Comm. Heat and Mass Transfer 36 624-631.

Jha,B.K., and Ajibade,A.O., (2010),Free convection flow between vertical porous plates with periodic heat input, Z. Angew. Maths. Mech., 90, 185-193.

Jha,B.K., Daramola, D., and Ajibade, A.O., (2013),Steady fully developed mixed convection flow in a vertical parallel plate microchannel with bilateral heating and filled with porous material, IMechE Part E: J Process Mechanical Engineering, Vol 227(1),56-66.

Jha,B.K., and Aina Babatunde, (2018) Role of suction/injection on steady fully developed mixed convection flow in a vertical parallel plate microchannel, Ain shams Engineering Journal, 9(4)., 747-755

Kavehpour,H.P., Faghri, M., and Asako, Y. , (1997), Effects of Compressibility and Rarefaction on Gaseous Flows in Microchannels, Numer. Heat Transfer Part A, 32, 677-696.

Kaviany,M., (1985), Laminar flow through a porous channel bounded by isothermal parallel plates, Int. J. Heat Mass Transfer, 28, 851-858.

Kou, H. S., and Lu, K. T., (1993), Combined Boundary and Inertia Effects for fully developed Mixed Convection in a vertical channel Embedded in porous media, Int. Comm. Heat Mass Transfer, 20, 333-345.

Kuznetsov, A.V.,(1998) Analytical study of fluid flow and heat transfer during force convection in a composite channel partially filled with Brinkman-Forchheimer porous medium, Flow, Turbulence and Combustion, 60, 173-192

Kuznetsov,A.V., and Nield, D.A., (2009), Thermally Developing Forced Convection in a Porous Medium Occupied by a Rarefied Gas; Parallel Plate Channel or Circular Tube with Walls at Constant Heat Flux, Transp. Porous Med., 76, 345-362.

Mishra, A. K., Paul, T., and Singh,A.K., (2002), Mixed convection flow in a porous medium bounded by two vertical walls, Forschung3im Ingenieurwesen Springer-Verlag, 67 198-205.

Purcell, E.M., (1977), Life at low Reynold number, American Journal of Physics, 45, 3-11

Renken,K.S., and Poulikakos, D.,(1988), Experiment and analysis of forced convective heat transport in a packed bed of spheres, Int. J. Heat Mass Transfer, 31, 1399-1408.

Sheremet,M.A., Rosca,N.C., Rosca, A.V., Pop,I,(2018), Mixed convection heat transfer in a square cavity filled with nanofluid with suction/injection effect, Computer and Mathematics with Applications 76,2665-2677.

Shojaefard, M. H., Noorpoor,A.R., Avanesians,A., and Ghaffapour,M., (2005), Numerical investigation of flow control by suction and injection on a subsonic airfoil, Am. J. Appl. Sci., 20(10), 1474-1480

Tuckerman,D.B., and Pease, R.F.W., (1981),High Performance heat Sinking for VLSI,IEEE Electron Device Lett, 2(5), 126-129.

Vafai,K., and Kim, S.J., (1989), Force convection in a channel filled with a porous medium: An exact solution, Trans. ASME- J. Heat Transfer, 111, 1103-1106.

Wang,C.L., and Liu, F.,(2007), Forced convection in a slightly curved microchannel, Int. Journal of Heat and Mass Transfer, 50, 881-896.

Wen-Mon, Y., and Hung-Yi, Li., (2001), Radiation effect on Mixed Convection Heat Transfer in Vertical Square duct, Int. J. Heat Mass Transfer, 44, 1401-1410.

APPENDICES

$$a1 = \sqrt{\left(\frac{S}{2M}\right)^2 + \frac{1}{MDa}}, x_1 = (SPr)^2 - \frac{S^2Pr}{M} - \frac{1}{(MDa)}, C4 = \frac{b_1\frac{dp}{dx} - b_2\frac{Gr}{Re}}{q_5},$$

$$C_3 = \left(x_2\frac{dp}{dx} - x_4\frac{Gr}{Re} + C_4x_3b\right)q_3, x_2 = Dacosh\left(\frac{S}{2M}\right), x_3 = \frac{C_2}{x_1g}cosh\left(\frac{S}{2M} - SPr\right),$$
$$x_{3_a} = Kn\frac{C_2}{x_1g}SPrsinh\left(\frac{S}{2M} - SPr\right)$$

$$x_{3b} = Kn\frac{S}{2M}sinh(a_1), q_3 = \frac{1}{cosh(a1) + a_1Knsinh(a1)}, q4 = \frac{1}{sinh(a1) + a_1Kncosh(a1)},$$
$$x_4 = C_1x_2 - x_3 + x_{3a}, x_5 = Dasinh\left(\frac{S}{2M}\right), x_6 = \frac{C_2}{x_{1g}}sinh\left(\frac{S}{2M} - SPr\right),$$
$$x_{6a} = Kn\frac{C_2}{x_{1g}}SPrcosh\left(\frac{S}{2M} - SPr\right),$$

$$x_{6b} = Kn\frac{S}{2M}cosh(a_1), x_7 = C_1x_5 - x_6 + x_{6_a}, q_5 = 1 - (q_3x_{3b}q_4x_{6b}),$$
$$b_1 = q_4(x_5 + q_3x_{6b}x_2), b_2 = q_4(x_7 + q_3x_{6b}x_4), x_8 = \frac{sinh\left(a_1 - \frac{S}{2M}\right)}{a_1 - \frac{S}{2M}} + \frac{sinh\left(a_1 + \frac{S}{2M}\right)}{a_1 + \frac{S}{2M}},$$

$$x_9 = \frac{sinh\left(a_1 - \frac{S}{2M}\right)}{a_1 - \frac{S}{2M}} - \frac{sinh\left(a_1 + \frac{S}{2M}\right)}{a_1 + \frac{S}{2M}}, x_{10a} = x_9 + x_8q_3x_{3b}, x_{10} = 2DaC_1 - \frac{2C_2sinh(SPr)}{x_{1_g}SPr},$$
$$x_{11} = x_{10} - \left(x_8q_3x_4 + \frac{x_{10_a}b_2}{q_5}\right), x_{12} = x_8x_2q_3 - 2Da + \frac{x_{10_a}b_1}{q_5}, x_{13} = \frac{C_2SPrexp(SPr)}{x_1M},$$
$$x_{14} = exp\left(\frac{S}{2M}\right)\left(\frac{S}{2M}cosh(a1) + a_1sinh(a1)\right)$$

$$x_{15} = exp\left(\frac{S}{2M}\right)\left(\frac{S}{2M}sinh(a_1) + a_1cosh(a_1)\right), x_{16} = \frac{b_1x_{15}}{q_5} - q_3x_{14}\left(x_2 + \frac{x_{3_b}b_1}{q_5}\right),$$
$$x_{17} = x_{13} - \frac{x_{15}b_2}{q_5} + x_{14}q_3\left(x_4 + \frac{x_{3b}b_2}{q_5}\right), x_{18} = -exp\left(\frac{-S}{2M}\right)\left(\frac{S}{2M}cosh(a_1) - a_1sinh(a_1)\right)$$

$$x_{19} = -exp\left(\frac{-S}{2M}\right)\left(\frac{S}{2M}sinh(a_1) - a_1cosh(a_1)\right), x_{20} = \frac{C_2SPrexp(-SPr)}{x_1M}x_{21a} = x_{19} + x_{18}x_{3b}q_3,$$
$$x_{21} = \frac{b_1x_{21a}}{q_5} + x_2x_{18}q_3x_{22} = x_{20} - \frac{b_2x_{21a}}{q_5}$$